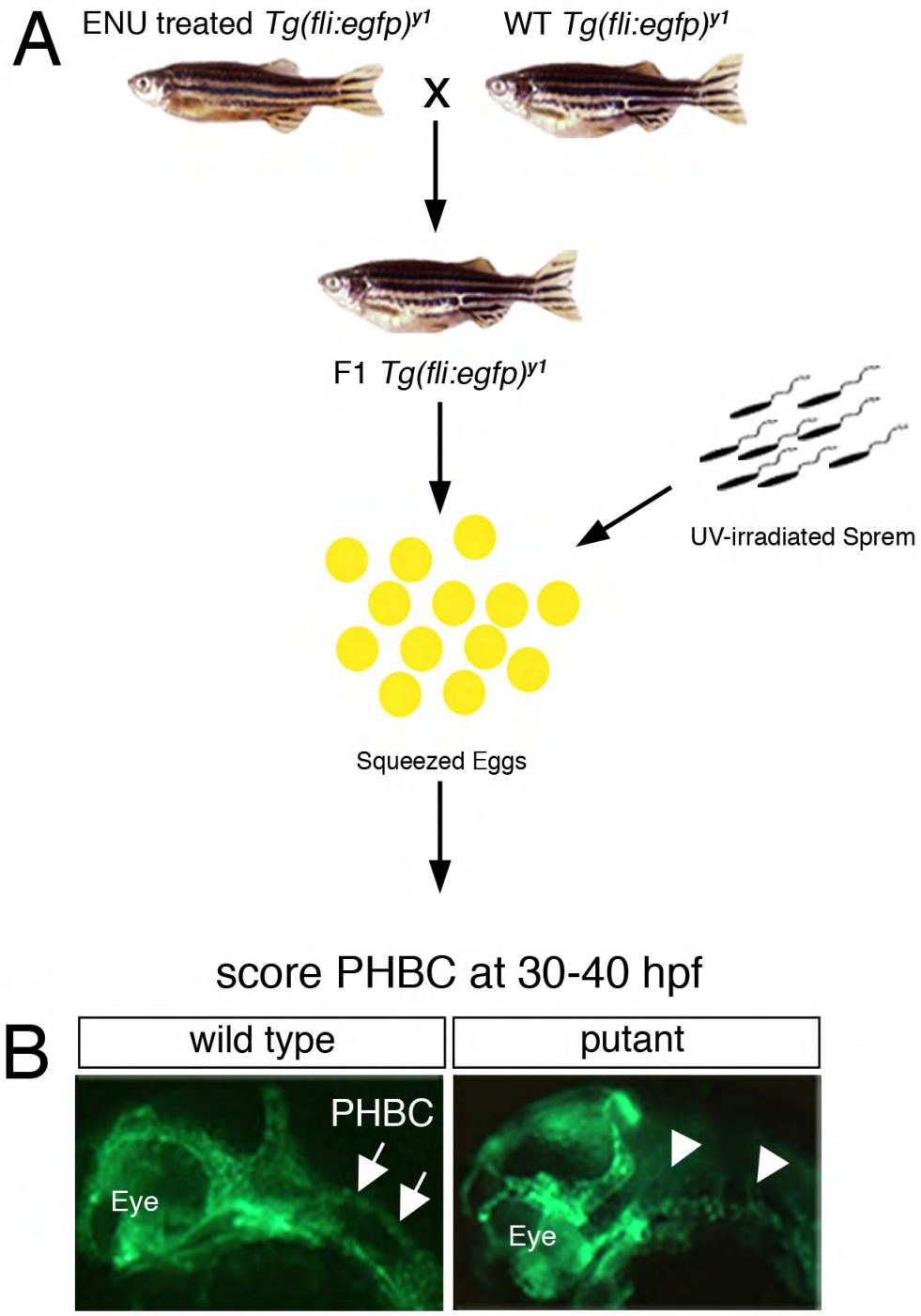

Fig. S1. Transgenic haploid screen in *Tg(fli1a:egfp)^{y1}* zebrafish to identify mutants affecting Vegfc/Flt4 signaling. (**A**) *Tg(fli1a:egfp)^{y1}* males were treated with N-ethyl-N-nitrosourea (ENU) to induce mutations in the pre-meiotic germline and subsequently outcrossed to wild-type *Tg(fli1a:egfp)^{y1}* females to establish F1 families. Eggs from individual F1 females were fertilized *in vitro* with UV-irradiated sperm from wild-type males to generate haploid embryos. (**B**) Epifluorescence images of cranial blood vessels in *Tg(fli1a:egfp)^{y1}* haploid embryos. (Left) Normal primordial hindbrain channel (PHBC) formation (arrows) at 28 hpf. (Right) Putative mutant embryo ('putant'), which failed to form a PHBC (arrowheads denote location where PHBC normally forms).

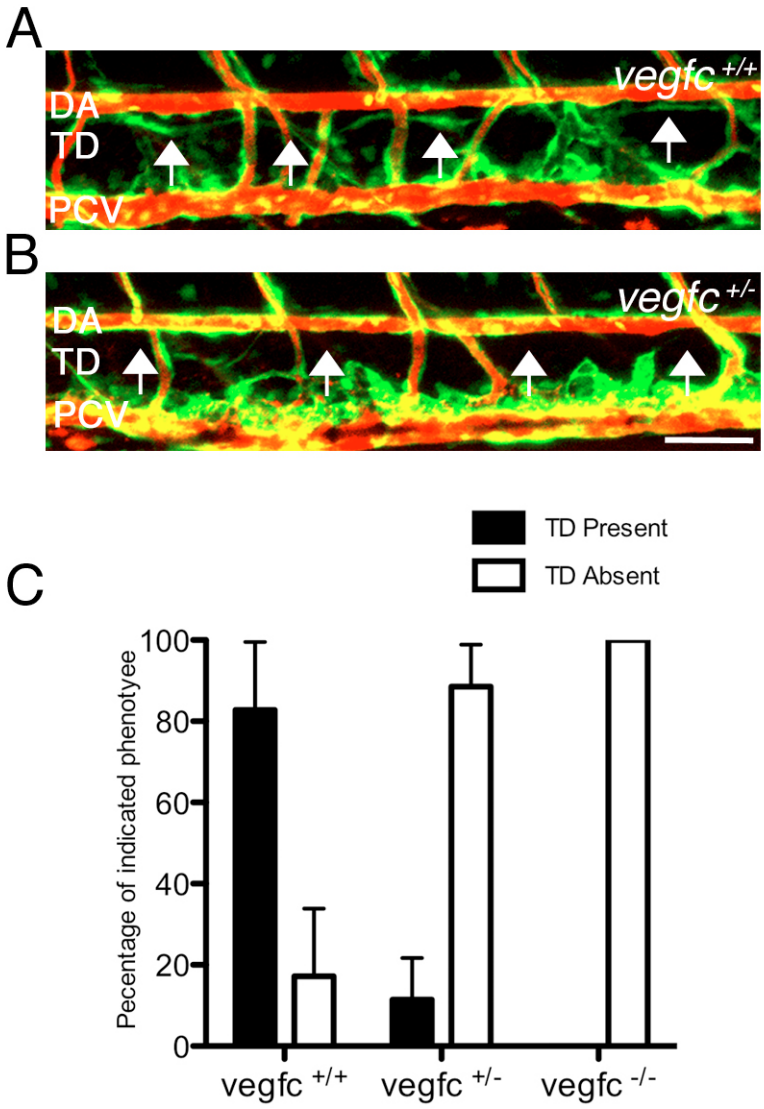

Fig. S2. Decreased thoracic duct formation in *vegfc*^{um18} heterozygous embryos. (**A**,**B**) Confocal microangiographs of trunk blood vessels in *Tg(fli1a:egfp)*^{y1} larvae at 5 dpf in progeny from a *um18* carrier incross. Microangiography dye is pseudocolored red. (A) Normal TD formation in a wild-type embryo. (B) Loss of TD in *vegfc*$^{um18/+}$ heterozygous embryo. The normal location of the thoracic duct (TD) is indicated by arrows. Lateral view, dorsal is up and anterior to the left. DA, dorsal aorta; PCV, posterior cardinal vein. (**C**) Quantification for presence of TD in embryos of the indicated genotype. Scale bar: 25 μm.

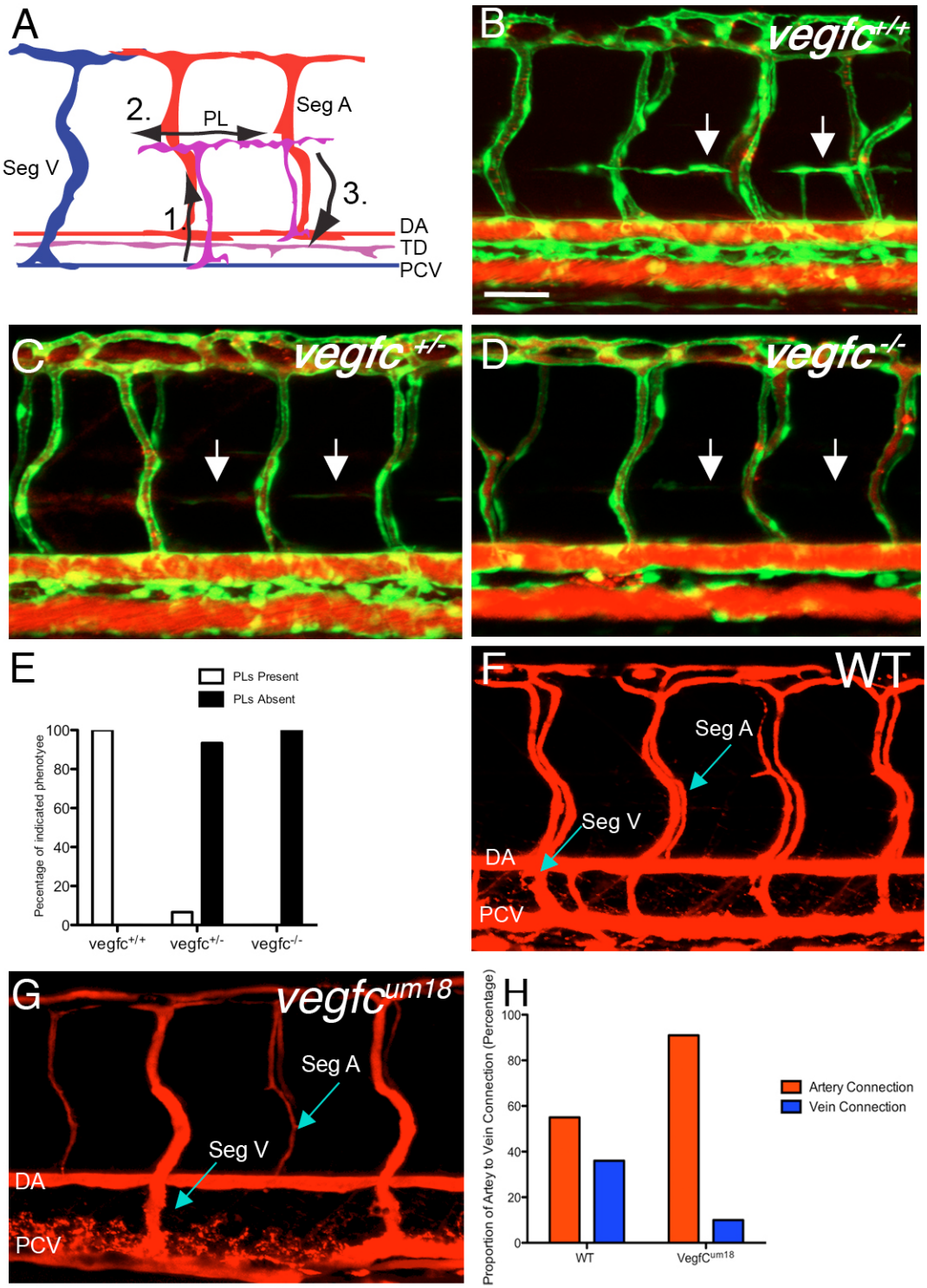

Fig. S3. *Vegfc*^{um18} mutants display primary defects in lymphatic progenitor and vein sprouting. (**A**) Diagram describing lymphatic vessel formation in zebrafish. (1) Dorsal sprouting of parachordal lymphangioblasts (PLs) from the posterior cardinal vein (PCV) at 1.5-2 dpf. (2) Ventral migration of PLs along the horizontal myoseptum. (3) Ventral migration of PLs to a position between the dorsal aorta and posterior cardinal vein to form the TD. (**B-D**) Confocal microangiographs of trunk blood vessels in *Tg(fli1a:egfp)*^{y1} embryos at 2 dpf. Anterior is to the left, dorsal is up. White arrows indicate position where PLs normally form. (B) Wild-type embryo. (C) *vegfc*$^{um18/+}$ heterozygous embryo. (D) *vegfc*^{um18} homozygous mutant embryo. (**E**) Quantification of PL formation. Values indicate the percentage of embryos of the indicated genotype that display either presence or absence of PLs. (**F**,**G**) Confocal microangiographs of trunk blood vessels at 3 dpf. Anterior is to the left, dorsal is up. DA, dorsal aorta; PCV, posterior cardinal vein; SegA, segmental artery; SegV, segmental vein. White arrowheads indicate SegA. (F) Wild-type sibling embryo. (G) Homozygous *vegfc*^{um18} mutant embryo. (**H**) Quantification of percentage artery and vein connections in wild-type and *vegfc*^{um18} mutant embryos. Mutants were identified as those lacking a PHBC at 30 hpf. At 3 dpf, embryos of both phenotypic classes were scored for the connection of intersegmental vessel to either DA or PCV based on blood flow. The values shown are based on the average of three independent experiments. Scale bar: 25 μm.

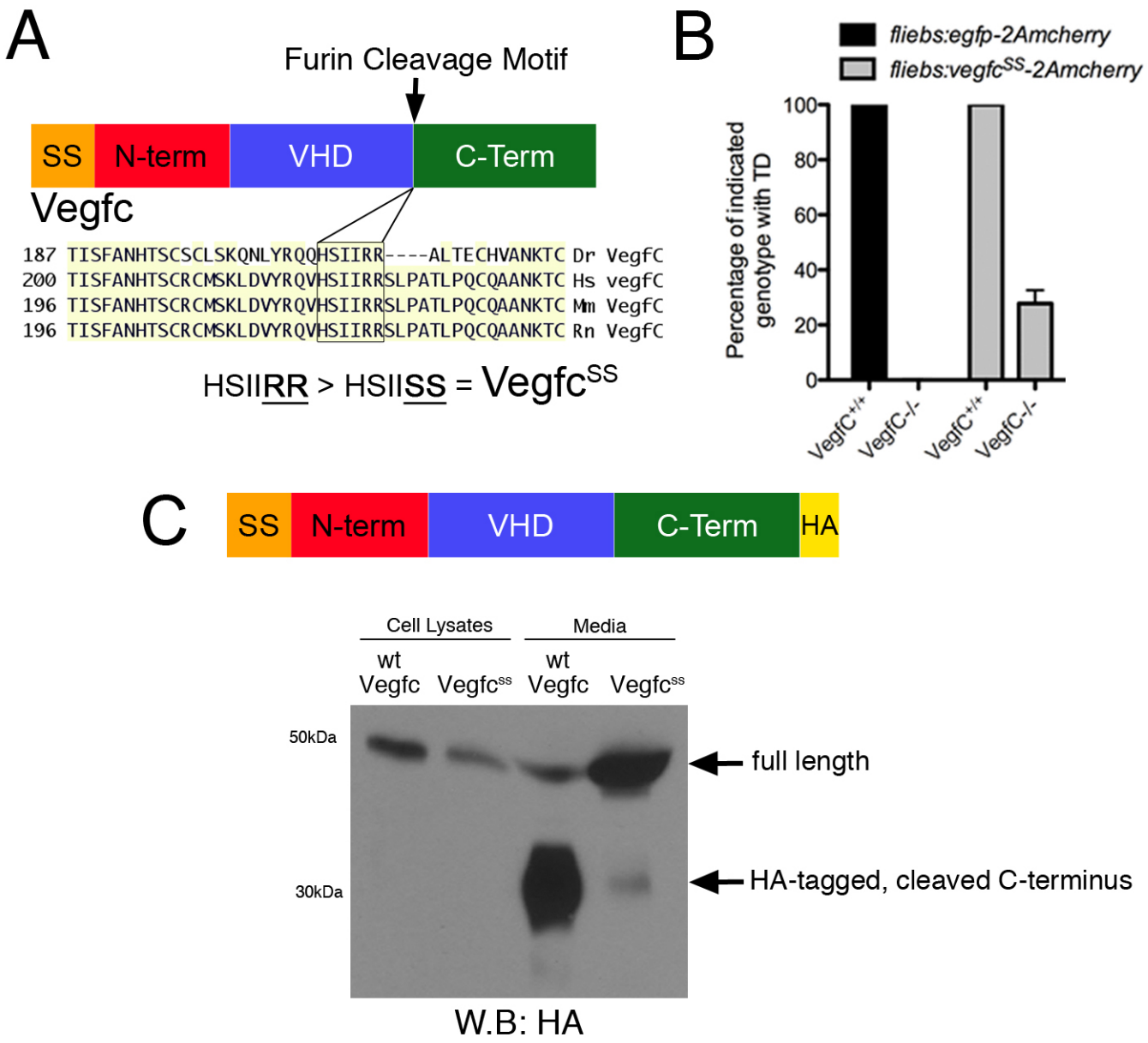

Fig. S4. A furin-resistant form of Vegfc (Vegfc^{ss}) is secreted and can partially rescue lymphatic development in *vegfc^{um18}* mutant embryos. (**A**) Vegfc structure showing location of the furin cleavage domain and the conserved amino acid sequences from zebrafish (Dr), human (Hs), mouse (Mm) and rat (Rn) Vegfc proteins. The amino acid substitutions to prevent furin cleavage are shown. (**B**) The proportion of embryos with indicated genotypes that displayed TD formation following injection of an endothelial driven *egfp-2Acherry* or *vegfc^{ss}-2Acherry* transgene. (**C**) Zebrafish Vegfc structure showing location of the hemagglutinin (HA) epitope tag at the C-terminus used to detect expression of furin-resistant Vegfc (Vegfc^{ss}). Western blot shows expression of wild-type zebrafish Vegfc or Vegfc^{ss} in cell lysates or extracellular media from transiently transfected NIH3T3 cells. In cell lysates, full-length Vegfc can be detected in both cases. Interestingly, we can detect a small amount of full-length wild-type Vegfc in the medium, along with the C-terminal domain that has been cleaved. Furthermore, we are able to detect furin-resistant Vegfc^{ss} in the medium, the vast majority of which remains unprocessed.

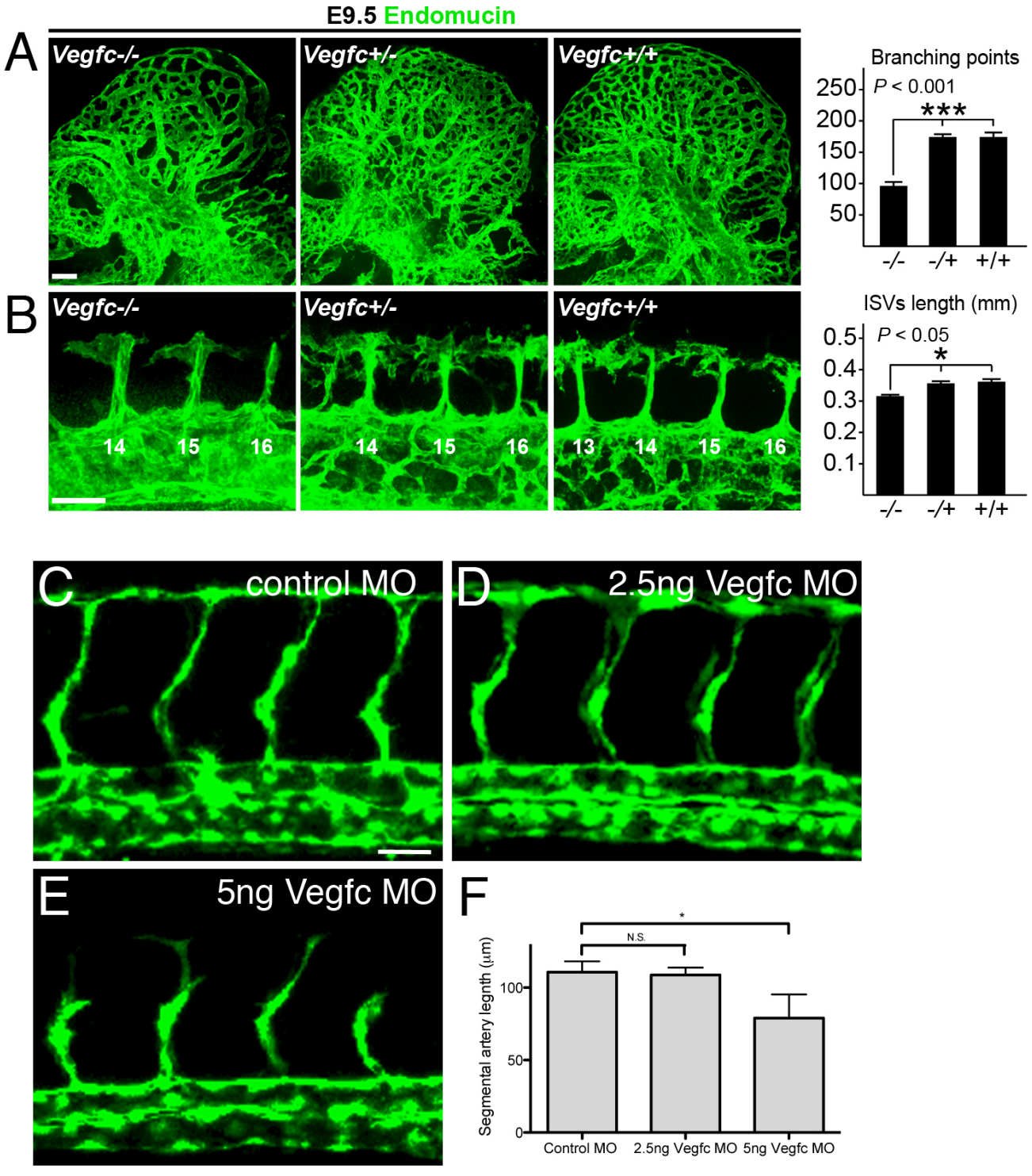

Fig. S5. Developmental angiogenesis defects in *vegfc*-deficient mouse and zebrafish embryos. (**A**,**B**) Confocal micrographs of mouse embryos of the indicated genotype at E9.5 stained with endomucin to visualize endothelial cells. (A) Cranial vessels (left) and quantification of branching points (right). (B) ISVs (left) and quantification of added ISV length, between somites 14-16 (right). *n*=3. (**C-F**) Confocal micrographs of *Tg(fli1a:egfp)*^{y1} wild-type zebrafish embryos at 30 hpf injected with (C) 5 ng control, (D) 2.5 ng Vegfc or (E) 5 ng Vegfc MO. Lateral views, dorsal is up, anterior to the left. (F) Quantification of ISV length in MO-injected *Tg(fli1a:egfp)*^{y1} embryos. **P*<0.05; N.S., not significant. Scale bars: 100 μm in A,B; 25 μm in C-E.

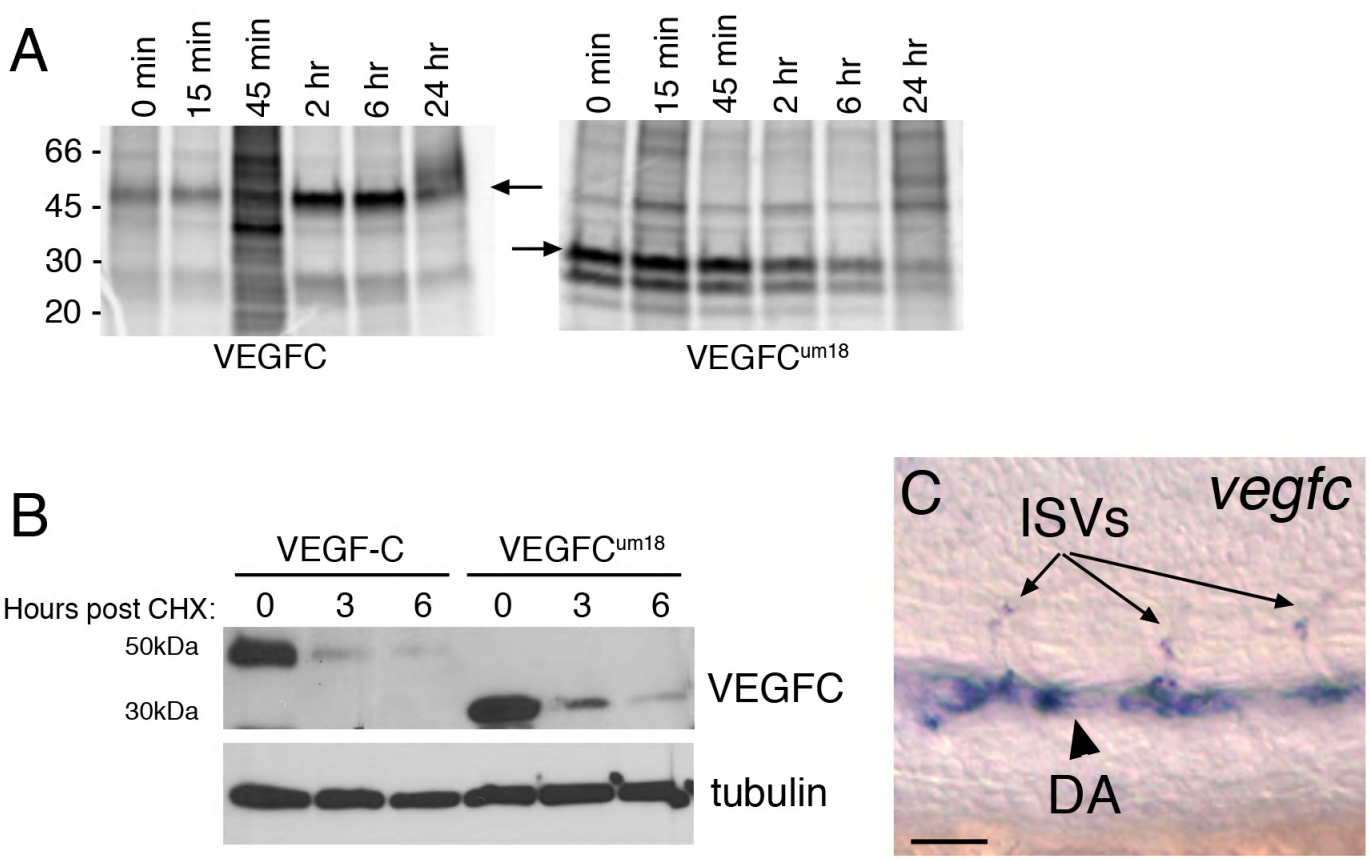

Fig. S6. *um18* does not affect VEGFC stability. (**A**) Visualization immunoprecipitated from VEGFC or VEGFC^{um18} from transfected HEK293T cell lystaes following a 2-hour pulse with radiolabeled Met and Cys, and chase with non-radiolabeled amino acids for the indicated time. Arrows indicate wild type (left) and truncated (right) VEGFC. (**B**) Western analysis of HEK293T cells expressing either VEGFC or VEGFC^{um18} and treated with cycloheximide (CHX). Cells grown in 6-well plates were transfected with 360 ng pSport6hVEGFC or pCSVEGC^{um18} and individual wells treated for 3 or 6 hours with cycloheximide (Sigma; 50 µg/ml final concentration). (**C**) *vegfc* expression in the dorsal aorta (DA) and intersegmental vessels (ISVs) at 24 hpf as detected by whole-mount *in situ* hybridization using a DIG-labeled antisense riboprobe. Lateral view, anterior to the left, dorsal is up. Scale bar: 25 µm.

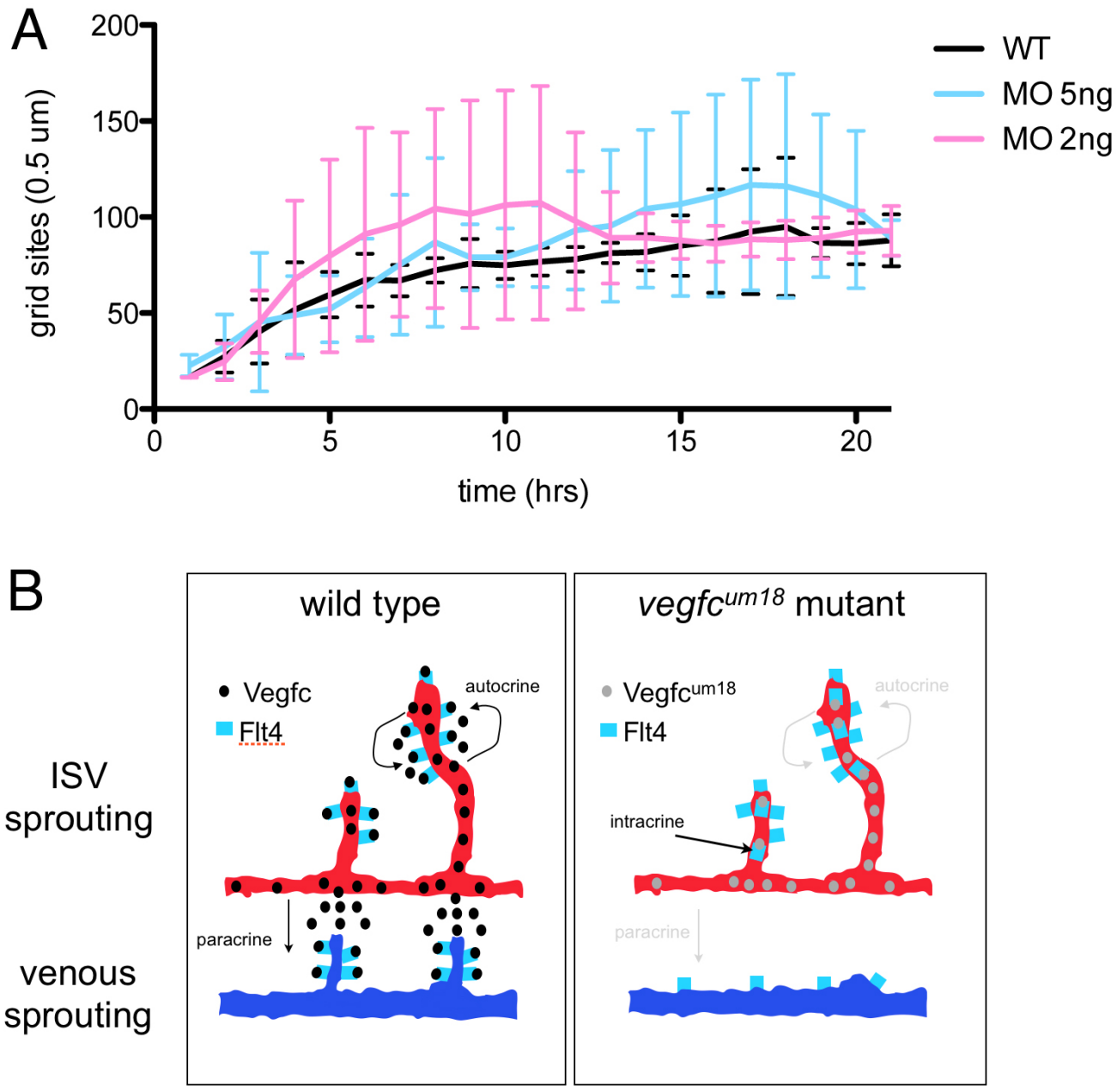

Fig. S7. Simulating a direct effect on Notch and a model for Vegfc function during vascular development. (**A**) ISV growth in simulations where Vegfc was predicted to have a direct effect on Notch signaling (Type 1 mechanism, see Materials and methods). (**B**) Model of autocrine and paracrine signaling roles for Vegfc during ISV sprouting and venous sprouting, respectively. In *vegfc*^{um18} mutants, a block in secretion prevents Vegfc from acting as a paracrine factor to promote sprouting of lymphatic progenitors from the posterior cardinal vein. The Vegfc/Flt4 autocrine loop required for ISV sprouting would likewise be affected. However, compensatory intracrine activation of Flt4 would allow normal ISV sprouting to proceed.

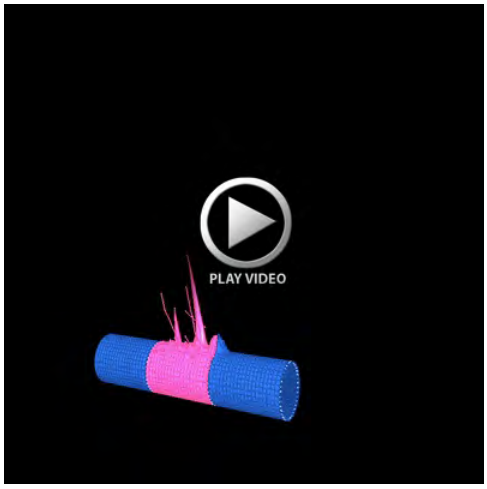

Movie 1. Simulation of a control tip cell migrating in a simulated ISV environment.

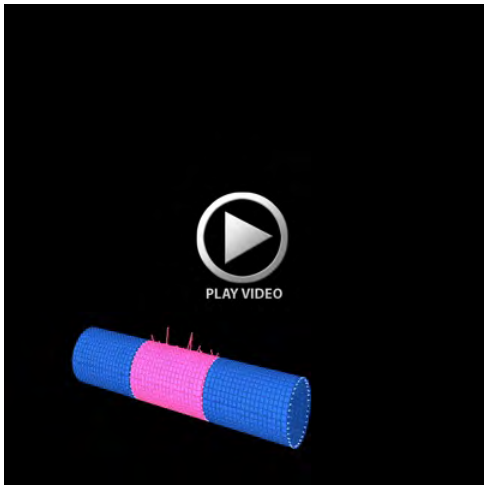

Movie 2. Simulation of a Vegfc MO (5 ng) tip cell migrating in a simulated ISV environment with settings that match mechanism Type 2b, which affects filopodia persistence.

Movie 3. Simulation of a wild-type vessel comprising seven cells with randomized veil advance. Color represents Vegfr2 receptor levels: pink, high; purple, low.

Movie 4. Simulation of a vessel with Vegfc MO (5 ng) using the matching mechanism for Vegfc (which increases filopodia persistence). Tip cells are selected more slowly as the cells randomly pull back migratory protrusions under the MO, affecting their position in the VEGF gradient and thus their ability to inhibit their neighbors consistently. This simulation predicts that tip cells would be seen to extend and then retract a number of times until a clear selection is made. Color represents Vegfr2 receptor levels: pink, high; purple, low.

Movie 5. Example of intersegmental vessel sprouting in a *Tg(fli1a:egfp)^{y1}* embryo injected with 5 ng control MO. Images were acquired by two-photon microscopy.

Movie 6. Example of intersegmental vessel sprouting in a *Tg(fli1a:egfp)^{y1}* embryo injected with 5 ng Vegfc MO. Images were acquired by two-photon microscopy.

Table S1. PCR primers used in this study

	Forward primer (5'-3')	Reverse primer (5'-3')
Mapping		
Z25069	AGTTACTTGCGATCCGACCA	TCACTGGTAAACACCCCTACA
Z11618	TGAGTGGGTGTAGAGGGACA	GATAAGGGGCCTCTTGGTTC
Z26040	CCAGAGAACTCCACTTGTGC	CCCAACTCTGGTCACAATACAA
Z24128	CTCATCACCGCTGCAATAAA	ATCTTGTGGGAAACGAGTGG
Vegfc 3'UTR SNP	CCAACCAACAGTGCAGATG	GGTTCGAAATGAATGAGTTGC
vegfC int/ex 1	GGACCAGTACCGAAGTGACTTC	GCCGGTGATGTTGACTGTTGATG
vegfC int/ex 2	GCCATTCTGATTGTGTGACCGG	GGCCACCACTGAAATGCTTTAC
vegfC int/ex 3	GCCAAAGATTGTGTTGGCAGTA	GCGATACTCACTGCACCACC
vegfC int/ex 4	CCACATTTCATTTTGACATCCAGC	GGTGTTCCATTCGTGACTTGA
VegfC Int/ex 5	CCGCTTTCTCCAAGATATTTTC	ACTGTGTGTTCAGGACGTGC
VegfC Int/ex 6	GTATGAATTTTGGGTAGAACTGCTG	GCTGGAGAGAGTTTATCAGATTTG
VegfC Int/ex 7	CTGATTGTAGTTTTGACCCATGT	CCAGTTTCTCCATTGCTAGTCC
Cloning		
pME*vegfc*	GGGGACAAGTTTGTACAAAAAAGCAGGCTGGGCCACCATGCACTTATTTGGATTTTCTG	GGGGACCACTTTGTACAAGAAAGCTGGGTTTTAGTCCAGTCTTCCCCAGTA
pME*vegfc*^{um18}	GGGGACAAGTTTGTACAAAAAAGCAGGCTGGGCCACCATGCACTTATTTGGATTTTCTG	GGGGACCACTTTGTACAAGAAAGCTGGGTCTTGTTTTGACAAACAGCTGCAGG
pMT-Ex-zfVEGF-C-wt	GAGGATCCATTCGAGTCAAGTCACGACTAC	GGGCCCTCTAGACTCGAGCG
pMT-Ex-zfVEGF-C-um18		CTGCGGCCGCTTATTTTGACAAACAGCTGCAGGAAG
pME VEGF-CΔC	GGGGACAAGTTTGTACAAAAAAGCAGGCTGGGCCACC**ATG**CACTTGCTGGGCTTCTTCT	GGGGACCACTTTGTACAAGAAAGCTGGGTCTTATTTAGACATGCATCGGCAGG
pMEflt4 w/o stp	GCCACCATGAAGAGAGATTTTACGTTTTTCTG	CGTAAACGGCCTGGTCTGAG

Table S2. Calibrated parameters for computational simulation of ISV sprouting

	k1 (2ng)	k2 (5ng)	tip k1	stalk k1	tip k2	stalk k2
Experimental			65.22	91.30	46.67	100
Type 1a	–	1.3	–	–	39.76	97.59
Type 1b	9.2	9.8	66.23	93.51	40.31	97.71
Type 2a	–	1.8	–	–	45.76	98.30
Type 2b	0.001	0.005	61.19	88.06	44.26	98.36

Calibrated parameters for *k* in each of the four simulated autocrine mechanisms of Vegfc/Flt4 action giving matching results to experimental transplant data in a simulated chimera. Dashes indicate cases where no parameter could be found to closely match the experimental data.

Table S3. Vein and lymphatic vessel scoring in *vegfc*^{um18} embryos

	Genotype		
Phenotype	+/+	*vegfc*$^{+/um18}$	vegfc$^{um18/um18}$
PHBC+	18	23	11
PHBC–	0	1	12
PL+	8	4	0
PL–	10	20	23
TD+	10	2	0
TD–	8	22	23
	Total embryos:		*N*=65

Primordial hindbrain channel (PHBC) and thoracic duct (TD) formation in progeny of *um18* heterozygous carriers. Embryos were scored at 30 hpf for the presence of the PHBC and subsequently scored at 5 dpf for the presence of a TD. Embryos were subsequently genotyped for the *um18* mutation. *N*, total number of embryos scored. PL, parachordal lymphangioblast.

Table S4. Intersomitic vein formation in *vegfc*^{um18} embryos

	Genotype		
Phenotype	+/+	*vegfc*$^{+/um18}$	vegfc$^{um18/um18}$
ISVe+	22	19	1
ISVe–	0	5	17
	Total embryos:		*N*=65

Secondary intersegmental vein formation in progeny of *um18* heterozygous carriers.
Embryos were scored at 60 hpf for the presence or absence of intersegmental veins.
Embryos were subsequently genotyped for the *um18* mutation.
ISVe, intersegmental vein.